View metadata, citation and similar papers at core.ac.uk

brought to you by CORE

provided by UCL Discovery

jove Journal of Visualized Experiments www.jove.com

Video Article

Evaluation of Synapse Density in Hippocampal Rodent Brain Slices

Faye McLeod*[1], Aude Marzo*[1], Marina Podpolny[1], Soledad Galli[1], Patricia Salinas[1]

[1]Department of Cell and Developmental Biology, University College London

*These authors contributed equally

Correspondence to: Faye McLeod at f.mcleod@ucl.ac.uk, Aude Marzo at a.marzo@ucl.ac.uk

URL: https://www.jove.com/video/56153
DOI: doi:10.3791/56153

Keywords: Neuroscience, Issue 128, Neurons, synapses, brain slices, immunofluorescence, hippocampus, mouse, rat, vGlut1, PSD-95, vGAT, gephyrin

Date Published: 10/6/2017

Citation: McLeod, F., Marzo, A., Podpolny, M., Galli, S., Salinas, P. Evaluation of Synapse Density in Hippocampal Rodent Brain Slices. *J. Vis. Exp.* (128), e56153, doi:10.3791/56153 (2017).

Abstract

In the brain, synapses are specialized junctions between neurons, determining the strength and spread of neuronal signaling. The number of synapses is tightly regulated during development and neuronal maturation. Importantly, deficits in synapse number can lead to cognitive dysfunction. Therefore, the evaluation of synapse number is an integral part of neurobiology. However, as synapses are small and highly compact in the intact brain, the assessment of absolute number is challenging. This protocol describes a method to easily identify and evaluate synapses in hippocampal rodent slices using immunofluorescence microscopy. It includes a three-step procedure to evaluate synapses in high-quality confocal microscopy images by analyzing the co-localization of pre- and postsynaptic proteins in hippocampal slices. It also explains how the analysis is performed and gives representative examples from both excitatory and inhibitory synapses. This protocol provides a solid foundation for the analysis of synapses and can be applied to any research investigating the structure and function of the brain.

Video Link

The video component of this article can be found at https://www.jove.com/video/56153/

Introduction

The human brain is composed of approximately 10^{14} synapses. Synapse number is tightly regulated during the development and maturation of the central nervous system (CNS). Throughout development, synapse number is modulated by synaptogenesis and pruning to form functional neuronal networks. Learning and memory are supported by the regulation of synapse number and strength, a process known as synaptic potentiation and depression[1]. Importantly, the stabilization of mature synapses is essential for maintaining neuronal network connections. Furthermore, deficits in synapse density have been reported at the early stages of neurodegenerative conditions such as Alzheimer's disease (AD)[2]. Therefore, the ability to accurately identify and evaluate synapse number is fundamental to the assessment of brain physiology and pathology.

The extreme density and compact nature of synapses make it challenging to estimate their precise number in intact brain areas. Chemical synapses in the CNS are made of two neurons in close apposition, separated by a synaptic cleft[3]. The pre-synaptic terminal, or synaptic bouton, emerges from an axon and consists of accumulated vesicles, which contain neurotransmitters that define the specificity of a synapse—namely, glutamate and gamma-aminobutyric acid (GABA) for excitatory and inhibitory synapses, respectively. The membranes of the vesicles contain vesicular transporters specific to each neurotransmitter: vesicular glutamate transporter (vGlut) for glutamate and vesicular GABA transporter (vGAT) for GABA. The post-synaptic terminal is a highly dense structure composed of multiple proteins, including receptors, adhesion molecules, and scaffold proteins. In excitatory synapses, post-synaptic density-95 protein (PSD-95) is the most abundant scaffold protein[4], modulating excitatory N-methyl-D-aspartate(NMDA-) and α-amino-3-hydroxy-5-methyl-4-isoxazolepropionic acid (AMPA-) receptor function, whereas gephyrin anchors inhibitory receptors to the inhibitory post-synaptic terminal[5]. Overall, the specificity of proteins to pre- and post-synaptic compartments aid in the differentiation and identification of synapse subtypes.

The evaluation of synapse number can be performed with different techniques. The most common is the use of electron microscopy (EM), which enables the analysis of the synapse in compact and intact brain areas with high magnification and resolution. However, this technique is very expensive, requires complicated sample preparation, and is very time consuming. Other techniques include the use of array tomography[6], which has a major disadvantage in that it requires specialized and expensive equipment to perform the analysis. Furthermore, transgenic lines expressing specific synaptic markers are useful at evaluating synapse number[7], but the generation of new lines can be restrictive and costly, and the overexpression of proteins may result in undesirable off-target phenotypes.

Due to these limitations and for simplicity, many researchers evaluate synapse number by examining total synaptic protein levels. However, synapse loss can be observed before substantial changes in protein, as structural synaptic remodeling results in the dispersal of pre- or post-synaptic apposition, with no degradation of synaptic proteins. Furthermore, in AD, synaptic protein levels are reduced following synapse

Copyright © 2017 Creative Commons Attribution-NonCommercial-NoDerivs 3.0 Unported License

degeneration or neuronal death[8,9]. The quantification of total levels does not enable this distinction. Thus, there is a need to develop a reliable, accessible, and accurate method for the evaluation of synapse number in the brain.

In this article, we describe how to thoroughly identify and determine the number of synapses using immunofluorescence microscopy in hippocampal rodent brain slices. The synapses are defined by the colocalization of pre- and post-synaptic markers which appear in a punctate distribution. We demonstrate the validity of this technique through the study of Wnt signaling in the brain. Wnts are secreted proteins important for the formation, elimination, and maintenance of synapses. The *in vivo* induction of a secreted antagonist of the Wnt cascade, Dickkopf-1 (Dkk1), leads to excitatory synaptic loss while preserving inhibitory synapses in the hippocampus[10]. We illustrate the identification and count of excitatory and inhibitory synapses in hippocampal slices from an adult mouse expressing Dkk1 and highlight the transferability of this technique to other types of tissue/culture preparations.

Protocol

All the experiments using mice and rats were approved and conducted using Schedule 1 procedures covered under the Home Office Animals (Scientific Procedures) act 1986. The artificial cerebrospinal fluid (ACSF) recipe can be found in **Table 1**.

1. Acute Hippocampal Slice Preparation

1. Remove the mouse brain as quickly as possible, using a spatula and sharp scissors to cut the skull, and place it in ice-cold, oxygenated (95% O_2, 5% CO_2), high-sucrose ACSF (~100 mL).
2. Place the mouse brain on a Petri dish and remove the cerebellum and a small section of the frontal cortex with a scalpel before hemisecting down the midline of the brain.
3. Place the two hemispheres on the side that was just cut and glue each hemisphere onto the stage of a vibratome.
4. Cut 200 - 300 µm-thick sections of the complete region of interest. In the case of the hippocampus, approximately 3 - 4 slices per hemisphere should be obtained.
5. Using a plastic Pasteur pipette, transfer the slices to a chamber submerged in oxygenated (95% O_2, 5% CO_2) ACSF. Maintain at 34 °C for 30 min.
   NOTE: The treatment of slices with active pharmacological agents, such as recombinant Dkk1 proteins, can be performed at this stage by adding the agents to the slice chamber.
6. Remove the slices from the chamber using a paintbrush, place them into a 24-well plate, and fix for 20 min to 1 h in 4% paraformaldehyde (PFA)/4% sucrose at room temperature (RT).
   Caution: PFA is toxic, wear appropriate protection.
7. Wash the slices three times in 1X PBS (10 min each).
   NOTE: The protocol can be paused here for 1 - 2 days, as long as the slices are kept at 4 °C in 1X PBS.

2. Immunofluorescence for Synaptic Markers

NOTE: The recipes of all buffers used can be found in **Table 2**.

1. Replace the PBS with blocking/permeabilizing buffer (**Table 2**) in the slice wells and incubate at RT for 4 - 6 h.
2. Dilute the polyclonal guinea pig antibody against vGlut1 at a 1:2,000 dilution in blocking/permeabilization buffer.
   NOTE: vGlut1 is a marker for pre-synaptic excitatory terminal visualization. For post-synaptic excitatory synapse identification, use a polyclonal antibody against PSD-95 and dilute 1:500 in the same solution. Use a minimum volume of 300 µL in each well. To identify the anatomical location of the hippocampus, use an antibody that can also identify the neuronal structure, such as MAP2 or Tubulin. Work out the correct concentrations of all primary antibodies for the synaptic markers of choice (pre- and post-synaptic) and dilute in fresh blocking/permeabilizing buffer.
3. Incubate the slices in the primary antibody solution overnight (or for 1 - 2 days) at 4 °C. Use a shaking platform with vigorous movement.
4. Wash the slices three times in PBS (10 min each).
5. Dilute the appropriate secondary antibodies 1:500 in blocking buffer. For example, when using the vGlut1 guinea pig antibody, apply a secondary antibody that recognizes the guinea pig component (*e.g.,* donkey anti-guinea-pig) conjugated to a specific fluorophore. When using the PSD-95 rabbit antibody, apply a secondary antibody that recognizes the rabbit component (*e.g.,* donkey anti-rabbit) conjugated to a different specific fluorophore.
6. Incubate the slices in this solution for 2 - 3 h at RT. Ensure that the slices are protected from the light, as secondary antibodies are light sensitive.
7. Wash the slices three times in PBS (10 min each).
8. Carefully remove the slices from the 24-well plate using a paintbrush and place them evenly onto pre-labelled glass slides. Add a drop of mounting medium on top of each slice and then gently place a glass coverslip on top of the slices. Avoid the formation of air bubbles. Take care to use enough mounting medium (300-400 µL), as an insufficient amount may lead to dry slices.
9. Leave to dry for a minimum of 1 - 2 days at RT and keep the slides protected from light.
10. Store the slides at 4 °C in the short-term, but for long-term storage, keep them at -20 °C.

3. Confocal Image Acquisition and Analysis

1. **Imaging using confocal laser scanning microscopy.**
   1. Identify the region of the hippocampus to be imaged (*e.g.,* the cornu ammonis 1 and 3 (CA1, CA3) or the dentate gyrus (DG)) by means of a 10x or 20x objective.

Copyright © 2017 Creative Commons Attribution-NonCommercial-NoDerivs 3.0 Unported License

2. Change to a 40x or 63x oil-immersion objective to make sure the slice anatomy is intact by identifying continuous neurites and organized structure. Use a neuronal marker, such as MAP2, as a reference (**Figure 1A**).
3. Subsequently, switch to a 60x oil-immersion objective (NA = ~1.3 - 1.4) and adjust the settings for each channel to obtain optimal signal and contrast. Set the intensity of each laser to avoid the saturation of any pixels using a high-/low-contrast option.
   NOTE: These setting will depend on the microscope used, but refer to the **Table of Materials** for the laser power settings used in **Figure 2**, **Figure 3**, and **Figure 4**. For best results, use a 1024 x 1024-pixel resolution. The settings should remain constant throughout the different conditions of the same experiment. Additional zoom can be applied if required.
4. Evaluate the depth where the staining is even and acquire image stacks of at least 8 equidistant (250 nm) planes. Then take 3 adjacent representative images stacks from the same area of interest per slice.
   NOTE: The depth may vary from one slice to another but should always be approximately 2 - 5 µm from the surface of the slice.
5. Repeat the acquisition in at least 3 slices per condition and from 6 - 8 animals per treatment group.

2. **Image analysis.**
   NOTE: Use an automated image analysis software (See the **Table of Materials**). Note that some systems require a license, whereas others are free, such as ImageJ. The software used must analyze the images in 3D by taking into account all planes of the stack imaged. Refer to the **Table of Materials** for the details of the software used in the image analysis (**Figure 1**).
   1. Use a custom-based intensity threshold protocol to identify all synaptic puncta and neuronal markers, which are manually optimized and selected within the software [see **Table of Materials** for the specific software used in this protocol].
      NOTE: The software identifies a minimum and maximum intensity for each fluorophore and associates a percentage of intensity for each recognized object. Note that the percentage of intensity will vary according to the fluorophore used and the antibody against the synaptic marker.
   2. For synaptic markers, ensure that size filters (>0.1µm^3 and <0.8µm^3) are selected within the software and applied to the image. Adjust the parameters to ensure that the selected objects are not overlapping. Exclude any object that are too large or too small to be considered synaptic puncta (see **Figure 2B**).
      NOTE: Once optimized, the same threshold values are then applied to all images within a given experiment.
   3. Quantify the mean number, intensity, and volume of individual synaptic puncta (pre- or post-synaptic) using the optimized threshold protocols selected within the software. Normalize the puncta number to the volume of the image field (roughly 16,928 µm^3 in the system used here). Normalize the synaptic puncta intensity to the intensity of the reference neuronal marker.
      NOTE: Synapses are defined as the co-localization between both pre- and post-synaptic markers. Once the threshold protocols for pre- and post-synaptic puncta have been established, the software should identify the co-localization of synaptic puncta as the overlap of 1 pixel or more in a single plane.
      NOTE: For statistical analysis, confirm that all sets of samples follow normality and homogeneity of variance, as determined by Lilliefords and χ2-tests, respectively. Samples showing a normal distribution and homogeneity of variance should be analyzed with parametric tests, as described below. For example, excitatory synaptic puncta analysis should be performed using a one-way ANOVA with blocking and replication. Each individual experiment should be considered as a block; typically, there are three independent experiments, each with 1 - 3 mice from each condition.

Copyright © 2017 Creative Commons Attribution-NonCommercial-NoDerivs 3.0 Unported License

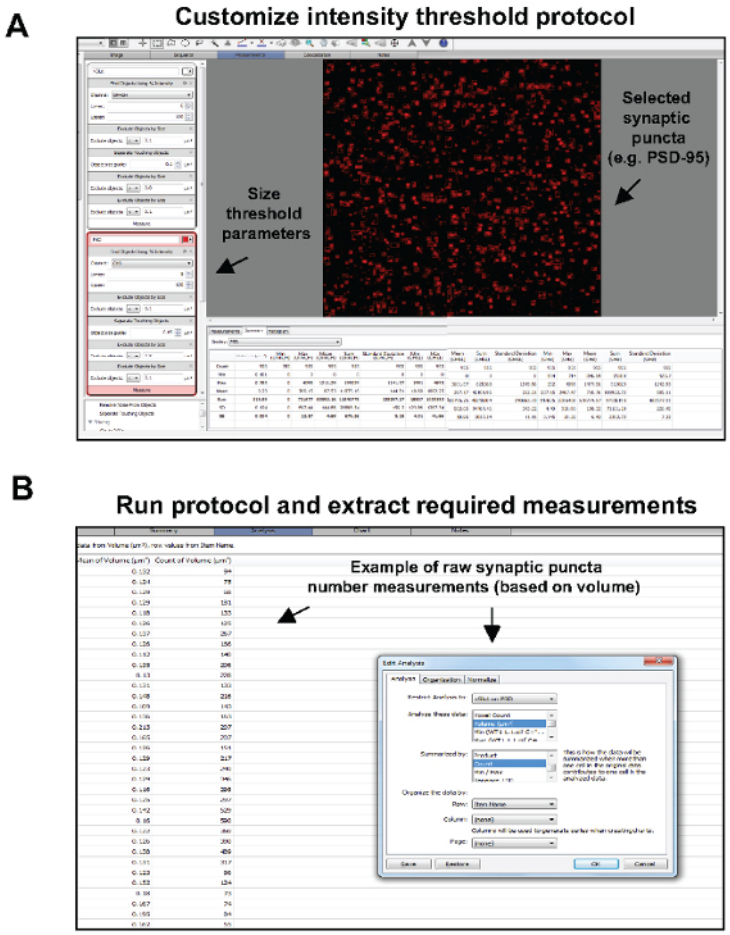

Figure 1: Analysis of synaptic puncta using the image analysis software. (**A**) Screenshot of the intensity threshold protocol customization. The example given is for PSD-95, in which the selected puncta have a defined size of >0.1 μm^3 and <0.8 μm^3 and present minimized overlapping objects. Note that the image shown is for one confocal plane to enable the easier visualization of synaptic puncta and accurate parameter selection. (**B**) Screenshot of the analysis output from the software (following the selection of the optimized protocol). An example of raw synaptic puncta number measurements based on the volume. These values are then exported to a spreadsheet software. Please click here to view a larger version of this figure.

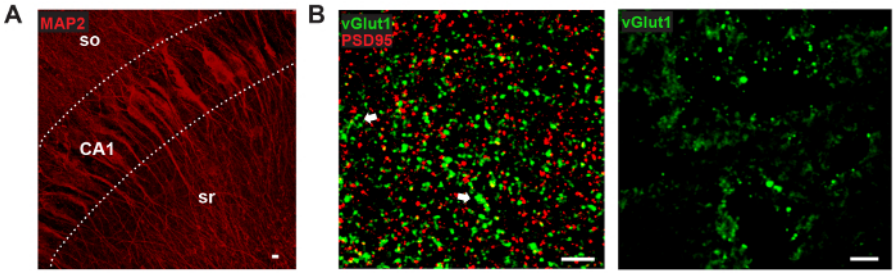

Figure 2: Quality check of the slice and parameter settings for synaptic puncta. (**A**) Representative confocal images (40x objective) of the region of interest: the CA1 stratum radiatum (sr) and stratum oriens (so) of a hippocampal slice are identified by MAP2 staining. Scale bar = 2 µm. (**B**) Confocal images (60x objective and an additional 1.3X magnification on the acquisition software) of the CA1 stratum radiatum, with excitatory markers-vGlut1 (green) and PSD-95 (red)-from hippocampal slices. Note the identification of clear pre- and post-synaptic puncta. Puncta larger than 0.8 μm^3 are excluded from the quantification (white arrows). Scale bar = 2 µm (C) Confocal images (60x objective and an additional 1.3X magnification on the acquisition software) of the CA1 stratum radiatum, with excitatory markers-vGlut1 (green)-from cryostat-cut hippocampal sections from entire brains fixed in PFA. Note the presence of large holes and irregular, clumped vGlut1 staining. Scale bar = 2 µm. Please click here to view a larger version of this figure.

Copyright © 2017 Creative Commons Attribution-NonCommercial-NoDerivs 3.0 Unported License

Representative Results

Synapse loss occurs early in neurodegenerative diseases such as AD and Parkinson's disease[2,11,12]. However, the molecular mechanisms underlying these deficits remain poorly understood. Deficiencies in Wnt signaling have been associated with AD[13,14,15,16,17]. Wnts are secreted glycoproteins and play an essential role in synapse formation and the modulation of synaptic transmission[18,19,20,21]. Recently, we identified Wnts as key regulators of synaptic maintenance in the mature nervous system[10,22]. To accurately study the impact of Wnt signaling on synapses in the hippocampus of genetically modified mice, we took advantage of a brain slice preparation and confocal microscopy to evaluate changes in synapse number. We identified healthy slices in which the structure was well preserved (**Figure 2A**). Moreover, the selection of synaptic puncta was carefully defined, with the exclusion of large stained objects probably representing aggregated proteins (**Figure 2B**). This criterion was applied to all images, with the same strict analysis parameters.

We used a transgenic model system that induces the expression of the secreted Wnt antagonist Dkk1 in adult mice (iDkk1) under tetracycline control (see the **Table of Materials**)[10,22]. We demonstrated that the blockade of Wnt signaling in the adult hippocampus triggers excitatory synapse loss specifically in the CA1 stratum radiatum region (**Figure 3**). **Figure 3A** illustrates representative confocal images of excitatory pre- and post-synaptic markers (vGlut1 and PSD-95, respectively) acquired from hippocampal slices of iDkk1 mice expressing Dkk1 for two weeks, as well as their respective controls. We analyzed these images using Volocity software and demonstrated a significant reduction in the number of excitatory synapses, quantified by the co-localization of vGlut1- and PSD-95-labeled puncta in the CA1 region of the hippocampus of iDkk1 mice following the induction of Dkk1 for two weeks (**Figure 3B**, *p <0.05; Kruskal-Wallis test; 6 mice per genotype). In the CA1 stratum radiatum, the excitatory synapse puncta number per 1,000 μm^3 was reduced from 500 in control mice to 300 in iDkk1 mice. In contrast, induced Dkk1 expression did not affect the number of inhibitory synapses (identified by the co-localization between the pre- and post-synaptic markers vGAT and gephyrin, respectively), as shown in **Figure 4A-B** (p >0.05; Kruskal-Wallis test; 3 mice per genotype).

Importantly, we performed a statistical power analysis to estimate the appropriate number of slices and animals required to generate these robust results. Using R, we calculated that approximately 35 slices per condition were needed (3 images x 3 slices x 6 animals = 36) to detect a large effect size (f = 0.4) with 80% confidence (power = 0.8) in a one-way ANOVA with blocking and replication, as described in step 3.2.6.

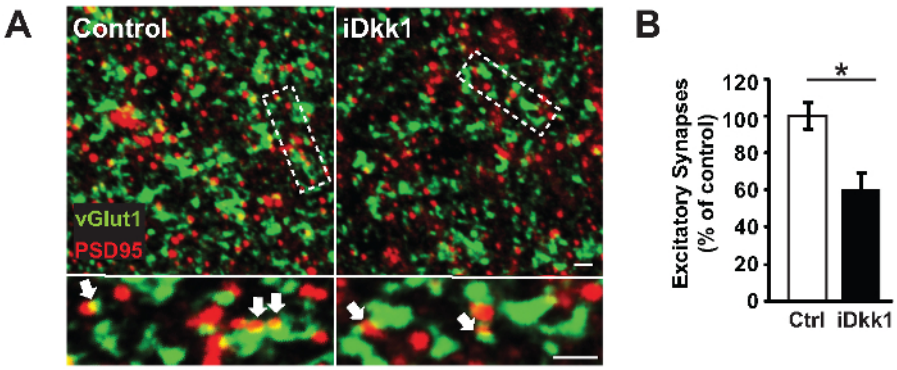

Figure 3: Loss of excitatory synapses in hippocampal slices from iDkk1 mice. (**A**) Representative confocal images of the CA1 stratum radiatum show excitatory synapses, identified by co-localization between vGlut1 and PSD-95 (white arrows). The lower panel represents a higher magnification of the highlighted rectangle. Scale bars = 2 µm. (**B**) The percentage of excitatory synapses between control and iDkk1 was quantified using software mentioned in **Table of Materials** (*p <0.05; Kruskal-Wallis test; 6 mice per genotype). The data are represented ± SEM. This figure has been modified from reference[10]. Please click here to view a larger version of this figure.

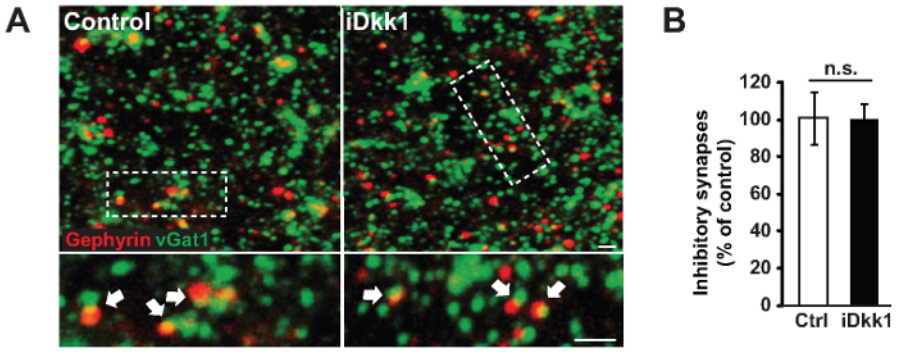

Figure 4:Inhibitory synapses are unchanged in hippocampal slices from iDkk1 mice. (**A**) Representative confocal images of the CA1 stratum radiatum of inhibitory synapses identified by the co-localization between vGAT and gephyrin (white arrows). The lower panel represents a higher magnification of the highlighted rectangle. Scale bars = 2 µm. (**B**) Percentage of inhibitory synapses between control and iDkk1 mice, as quantified using Volocity software (p >0.05; Kruskal-Wallis test; 3 mice per genotype). The data are represented ± SEM. This figure has been modified from reference[10]. Please click here to view a larger version of this figure.

Copyright © 2017 Creative Commons Attribution-NonCommercial-NoDerivs 3.0 Unported License

High Sucrose ACSF Components	Concentration	Notes
NaCl	75 mM	
$NaHCO_3$	25 mM	
KCl	2.5 mM	
NaH_2PO_4, $2H_2O$	1.25 mM	
Kynurenic acid	1.25 mM	
Pyruvic acid	2 mM	
EDTA	0.1 mM	
$CaCl_2$	1 mM	Add after oxygenation of solution
$MgCl_2$	4 mM	Add after oxygenation of solution
D-Glucose	25 mM	
Sucrose	100 mM	
Submerged chamber ACSF Components		
NaCl	125 mM	
$NaHCO_3$	25 mM	
KCl	2.5 mM	
NaH_2PO_4, $2H_2O$	1.25 mM	
$CaCl_2$	1 mM	Add after oxygenation of solution
$MgCl_2$	1 mM	Add after oxygenation of solution
D-Glucose	25 mM	

Table 1: ACSF composition.

Blocking/permeabilizing Buffer	Concentration	Notes
Donkey serum	10%	
Triton-X	0.50%	
PBS	1x	
10x PBS		**pH to 7.4**
NaCl	1.37 M	
KCl	27 mM	
NaH_2PO_4	100 mM	
KH_2PO_4	18 mM	
4% PFA/4% Sucrose		**pH to 7.4**
PBS	1x	Dilute from 10x
PFA	1.33 M	
Sucrose	117 mM	

Table 2: Buffers used for immunofluorescent staining.

Discussion

The precise evaluation of synapse number is essential to the field of neuroscience. Here, we show how to evaluate the density of synapses in the CA1 stratum radiatum region of hippocampal slices as a model system. The significance with respect to existing methods is demonstrated in our recent research article on the effect of Wnt deficiency in the hippocampus and where we also evaluated synapse number by single-section EM[10]. The magnitude of synapse loss are similar between single-section EM and the brain-slice method described here[10]. Thus, this finding demonstrates the accuracy and reliability of the technique.

Importantly, a limitation of both single-section EM and immunostaining synapses, as presented here, is the inability to accurately estimate the absolute synapse number for a specific brain region. Indeed, it is important to identify any global morphological changes, as changes in total volume could impact synaptic number. Another limitation is that certain antibodies are less efficient at staining intact brain regions, partially due to the extreme density of synaptic connections. We experienced higher-quality staining of vGlut1 and gephyrin using this slice preparation and subsequent PFA fixation for a maximum of 1 h, compared to immediate fixation of the entire brain in PFA (**Figure 2C**). The latter led to clumped

Copyright © 2017 Creative Commons Attribution-NonCommercial-NoDerivs 3.0 Unported License

synaptic staining, with holes in the tissue. Nonetheless, the vGlut1 antibody penetration is still restricted in both methods (a couple of tens of microns). We did not overcome this limitation, even with increased antibody incubation, but providing the antibody penetration is greater than the total depth that is imaged, there should be no influence on the final result. Furthermore, special care should be taken to ensure that the staining is even throughout the entire acquired stack.

In our study, we wanted to distinguish excitatory from inhibitory synapses. Consequently, we chose vGlut1/PSD-95 and vGAT/gephyrin, respectively, as these proteins are highly expressed in the adult mouse hippocampus and are specific to each synapse subtype[4,5]. Other excitatory and inhibitory synaptic markers could have been used to identify each respective synapse, such as receptors enriched at each synapse, including NMDA and AMPA receptors for excitatory and GABAA receptors for inhibitory synapses. Other neurotransmitters or neuromodulators can also be identified with our protocol, ensuring that specific antibodies are available, as shown for dopaminergic synapses in the striatum[22]. In addition, reducing the thickness of each slice to 120 µm can partially overcome the low quantity of samples obtained with acute slices, which is imperative for studies in small brain structures such as the amygdala.

Future applications of our protocol could be implemented in the study of different brain areas and disorders. For example, in the striatum (a region of the brain associated with Parkinson's disease), a combination of vGlut2/PSD-95 or vGlut1/PSD-95 could be used to differentiate between the excitatory synapses from afferents coming from the cortex or thalamus, respectively[22].

In conclusion, we have shown a reliable method to examine the number of synapses in brain tissues using pre- and post-synaptic markers to define a synapse. Critical steps include the preparation of good hippocampal slices, a fixation time of up to 1 h in PFA, the application of enough mounting medium, the use of reliable antibodies, appropriate image acquisition settings, and stringent synaptic puncta detection. Ultimately, this method is relatively quick and is easily reproducible by any laboratories that have access to a confocal microscope.

Disclosures

The authors have nothing to disclose.

Acknowledgements

This work was supported by the MRC, EU FP7, ARUK, Wellcome Trust, and Parkinson's UK. We would also like to thank Ms. Johanna Buchler for her contribution of confocal images and the members of the lab for their constructive input on the manuscript and methodology.

References

1. Malenka, R. C., Bear, M. F. LTP and LTD: an embarrassment of riches. *Neuron.* **44** (1), 5-21 (2004).
2. Arendt, T. Synaptic degeneration in Alzheimer's disease. *Acta Neuropathol.* **118** (1), 167-179 (2009).
3. Missler, M., Sudhof, T. C., Biederer, T. Synaptic cell adhesion. *Cold Spring Harb Perspect Biol.* **4** (4), a005694 (2012).
4. Chua, J. J., Kindler, S., Boyken, J., Jahn, R. The architecture of an excitatory synapse. *J Cell Sci.* **123** (Pt 6), 819-823 (2010).
5. Dobie, F. A., Craig, A. M. Inhibitory synapse dynamics: coordinated presynaptic and postsynaptic mobility and the major contribution of recycled vesicles to new synapse formation. *J Neurosci.* **31** (29), 10481-10493 (2011).
6. Jackson, R. J. *et al.* Human tau increases amyloid beta plaque size but not amyloid beta-mediated synapse loss in a novel mouse model of Alzheimer's disease. *Eur J Neurosci.* **44** (12), 3056-3066 (2016).
7. Heck, N. *et al.* A new automated 3D detection of synaptic contacts reveals the formation of cortico-striatal synapses upon cocaine treatment in vivo. *Brain Struct Funct.* **220** (5), 2953-2966 (2015).
8. Sultana, R., Banks, W. A., Butterfield, D. A. Decreased levels of PSD95 and two associated proteins and increased levels of BCl2 and caspase 3 in hippocampus from subjects with amnestic mild cognitive impairment: Insights into their potential roles for loss of synapses and memory, accumulation of Abeta, and neurodegeneration in a prodromal stage of Alzheimer's disease. *J Neurosci Res.* **88** (3), 469-477 (2010).
9. Harwell, C. S., Coleman, M. P. Synaptophysin depletion and intraneuronal Abeta in organotypic hippocampal slice cultures from huAPP transgenic mice. *Mol Neurodegener.* **11** (1), 44 (2016).
10. Marzo, A. *et al.* Reversal of Synapse Degeneration by Restoring Wnt Signaling in the Adult Hippocampus. *Curr Biol.* **26** (19), 2551-2561 (2016).
11. Zoghbi, H. Y., Bear, M. F. Synaptic dysfunction in neurodevelopmental disorders associated with autism and intellectual disabilities. *Cold Spring Harb Perspect Biol.* **4** (3) (2012).
12. Janezic, S. *et al.* Deficits in dopaminergic transmission precede neuron loss and dysfunction in a new Parkinson model. *Proc Natl Acad Sci U S A.* **110** (42), E4016-4025 (2013).
13. Caricasole, A. *et al.* Induction of Dickkopf-1, a negative modulator of the Wnt pathway, is associated with neuronal degeneration in Alzheimer's brain. *J Neurosci.* **24** (26), 6021-6027 (2004).
14. De Ferrari, G. V. *et al.* Common genetic variation within the low-density lipoprotein receptor-related protein 6 and late-onset Alzheimer's disease. *Proc Natl Acad Sci U S A.* **104** (22), 9434-9439 (2007).
15. Liu, C. C. *et al.* Deficiency in LRP6-mediated Wnt signaling contributes to synaptic abnormalities and amyloid pathology in Alzheimer's disease. *Neuron.* **84** (1), 63-77 (2014).
16. Purro, S. A., Dickins, E. M., Salinas, P. C. The Secreted Wnt Antagonist Dickkopf-1 Is Required for Amyloid beta-Mediated Synaptic Loss. *J Neurosci.* **32** (10), 3492-3498 (2012).
17. Rosi, M. C. *et al.* Increased Dickkopf-1 expression in transgenic mouse models of neurodegenerative disease. *J Neurochem.* **112** (6), 1539-1551 (2010).
18. Budnik, V., Salinas, P. C. Wnt signaling during synaptic development and plasticity. *Curr Opin Neurobiol.* **21** (1), 151-159 (2011).
19. Ciani, L. *et al.* Wnt signalling tunes neurotransmitter release by directly targeting Synaptotagmin-1. *Nat Commun.* **6**, 8302 (2015).

Copyright © 2017 Creative Commons Attribution-NonCommercial-NoDerivs 3.0 Unported License

20. Dickins, E. M., Salinas, P. C. Wnts in action: from synapse formation to synaptic maintenance. *Front Cell Neurosci.* **7** 162 (2013).
21. Inestrosa, N. C., Varela-Nallar, L. Wnt signalling in neuronal differentiation and development. *Cell Tissue Res.* **359** (1), 215-223 (2015).
22. Galli, S. *et al.* Deficient Wnt signalling triggers striatal synaptic degeneration and impaired motor behaviour in adult mice. *Nat Commun.* **5**, 4992 (2014).

Copyright © 2017 Creative Commons Attribution-NonCommercial-NoDerivs 3.0 Unported License